https://doi.org/10.5194/wes-2026-92
Preprint. Discussion started: 18 June 2026

eawe european academy of wind energy
Open Access WIND ENERGY SCIENCE DISCUSSIONS

Wind resource assessment in flow-distorting terrain: Techno-economic comparison of fixed-wing UAVs & profiling LiDAR

Phuong Anh Nguyen[1,2], Ewoud Vos[1], Danial Hassani[2]

[1] Hanze UAS, Entrance - Centre of Expertise Energy, Groningen, 9747 AA, The Netherlands
[2] Alveo AB, Stockholm, 138 33 Älta, Sweden

Correspondence to: Phuong Anh Nguyen (anhnp.hn13@gmail.com)

Abstract. This study conducts a head-to-head techno-economic comparison of vertical profiling Light Detection and Ranging (LiDAR) and fixed-wing Unmanned Aerial Vehicles (UAVs) deployments for wind resources assessment at a representative 120 MW onshore project in flow-distorting terrain in Germany. A simplified energy yield model and a Monte Carlo framework propagate literature-based measurement and flow model uncertainties through different measurement scenarios to the exceedance levels (P50, P90) of Annual Energy Production (AEP), Net Present Value (NPV) and Levelized Cost of Electricity (LCOE). The analysis shows that both technologies achieve similar point measurement uncertainties (±0.4-0.5 m/s, ±7-10°). The dominant lever for reducing AEP uncertainty and improving P90 is increased direct spatial coverage, not marginal gains in instrument accuracy. Under consistent cost and financing assumptions, UAV-based deployments deliver the largest P90 uplift, higher NPV and lower LCOE than LiDAR configurations.

1 Introduction

In line with Europe's strong commitment to achieving net-zero carbon emissions by 2050, a rapid expansion of renewable electricity is required, with onshore wind remaining to be the most immediately deployable option (Hernandez-Negron et al., 2023). While most onshore wind capacity has historically been installed in flat, lowland or coastal areas, new projects are increasingly expanded into non-uniform, mountainous and forested landscapes (Clifton et al., 2022). While these regions offer stronger wind resources, their flow-distorting characteristics are difficult to represent accurately using current measurement and modelling approaches. This creates not only engineering and logistical challenges but also significantly increases uncertainty in wind measurement and prediction (Clifton et al., 2022; Melani et al., 2023). Such uncertainty directly impacts energy yield estimation (Melani et al., 2023), and in turn, shapes project financing as well as overall economics (Clifton et al., 2016; Lee & Fields, 2021).

Specifically, as lenders and investors typically size debt and set pricing based on the risk associated with estimated annual energy production (AEP) and its exceedance levels (P50, P90) before making investment decisions (Melani et al., 2023). When uncertainty increases, perceived risk rises accordingly. As a result, debt capacity may be reduced and interest margins increased (Mora et al., 2019). Furthermore, inaccurate or overly uncertain AEP estimates can also lead to mispriced power purchase

https://doi.org/10.5194/wes-2026-92
Preprint. Discussion started: 18 June 2026

eawe european academy of wind energy
Open Access WIND ENERGY SCIENCE DISCUSSIONS

agreements (PPAs) and long-term economic underperformance (Barber et al., 2022). In flow-distorting terrain, reliable wind resource assessment (WRA) therefore becomes a critical bottleneck. The need for accurate, well-designed wind measurement campaigns is not merely technical, it is fundamental to reducing financial risk and ensuring project viability.

Conventional measurement practice for WRA relies on meteorological (met) masts. Masts provide traceable, long time series but are costly and difficult to install at modern hub heights and/or in rugged terrain (IEA Wind Task 36, 2022). Projects increasingly depend on single-point measurements that must be extrapolated vertically and horizontally across the wind farm (Clifton et al., 2022; Melani et al., 2023). Integrating with point-measurement practices for WRA, common flow models, used as spatial extrapolation tools, include linear models and computational fluid dynamics (CFD) approaches such as WAsP, RANS-CFD and large-eddy simulation (LES) (Barber et al., 2022; Clifton et al., 2016). There is, however, no community-wide best practice in complex terrain, as advanced models are computationally demanding, while their accuracy and uncertainty remain site dependent and subject to ongoing validation (Bechmann et al., 2011; Dörenkämper et al., 2020; Sheehan et al., 2022).

Remote sensing technologies have been introduced to overcome mast-installation challenges, with vertical profiling Light Detection and Ranging (LiDAR) now widely used for development campaigns in gentle terrain (Goit et al., 2019). Still, in flow-distorting terrain, profiling LiDAR data require site-specific corrections and must be translated spatially to turbine locations, again relying on flow models (Melani et al., 2023).

Unmanned aerial vehicles (UAVs) or drones have recently emerged as flexible platforms of sampling at hub height along extended flight tracks, improving representation of spatial heterogeneity (Dang et al., 2024). Long-endurance fixed-wing UAVs are stable in cruise and can cover larger areas, making them well suited for mapping mean wind conditions over the entire complex sites (Soltaninezhad et al., 2025), comparing to multirotor drones. Indirect wind estimation usually combines global navigation satellite system (GNSS) data, pitot tubes and inertial measurement units (IMUs) to reconstruct wind vectors along the flight path (Fu et al., 2025). For long-term or large-site measurements, fixed-wing platforms are generally preferred (Soltaninezhad et al., 2025). Recent developments seek to address these challenges, particularly through fixed-wing hybrid VTOL (vertical take-off and landing) UAVs, eliminating the need for catapults or runways (Hassani, 2023). Long-endurance fixed-wing UAVs, up to 6-9 hours per flight, have demonstrated fine-resolution wind and turbulence measurements in wind farm environments (Alaoui-Sosse et al., 2022; Hassani, 2023). Improvements in multi-sensor integration, data processing, as well as autonomous flight control and charging system further boost data reliability for long-term measurement and range (Alaoui-Sosse et al., 2022; Hassani, 2023). These innovations suggest UAVs could evolve into an even more competitive solution for wind measurement.

1.1 Motivation and problem statement

Accelerating the expansion of onshore wind in complex European terrain requires reducing measurement barriers at the wind resource assessment (WRA) stage. As met masts are often impractical, more flexible solutions are needed. Vertical profiling LiDARs and fixed-wing UAVs both offer greater deployment flexibility in such terrain, but neither is currently accepted as a

https://doi.org/10.5194/wes-2026-92
Preprint. Discussion started: 18 June 2026

eawe european academy of wind energy
Open Access WIND ENERGY SCIENCE DISCUSSIONS

standalone, bankable solution without site-specific validation and robust uncertainty quantification (Goit et al., 2019; Klaas-Witt & Emeis, 2022; Soltaninezhad et al., 2025). This lack of financial acceptance limits their ability to replace conventional measurement approaches.

Several studies report good agreement between fixed-wing UAVs, profiling LiDARs and reference systems across a range of terrains (e.g (Kim et al., 2016; Pauscher et al., 2016; Wildmann et al., 2014, 2017)). However, these validation efforts are typically conducted separately for each technology. Direct comparisons remain rare. For example, (Boventer et al., 2024) compares profiling LiDAR and fixed-wing UAV measurements at a mountainous site, but the datasets are not fully aligned: LiDAR data are averaged over 30 minutes, while UAV data are averaged over 10 minutes. Such asymmetries limit comparability. More broadly, the evidence base remains fragmented across methods, platforms and sites, and is largely framed in terms of technical measurement accuracy rather than its implications for energy assessment at farm-scale and project economics. Yet for investors and lenders, the critical question is not only whether a measurement is accurate, but how it affects annual energy production (AEP) uncertainty and, ultimately, financial outcomes.

This study addresses that gap through a head-to-head comparison of fixed-wing UAV and vertical profiling LiDAR deployments for a representative onshore wind project in flow-distorting terrain in Germany. Under consistent assumptions, it quantifies how alternative deployments of two technologies delivers measurement uncertainty and spatial extrapolation uncertainty to AEP (P50/P90 values), project net present value (NPV) and levelized cost of electricity (LCOE).

2 Methodology

A mixed-method approach, that combines a structured literature review, a quantitative case study and techno-economic comparison, is conducted (see Figure 1). The overall aim is to link empirically grounded measurement and flow model uncertainties to AEP uncertainty (P50/P90) and project-finance metrics for comparison. Finally, the robustness of key inputs and the internal logic of the model are examined through a sensitivity analysis.

2.1 Literature review

A literature review identifies the measurement accuracy and uncertainty of the two technologies in complex terrains, as well as the uncertainty of common flow models used in the WRA workflow. It focuses on onshore flow-distorting terrain (e.g. mountainous, hilly, and forested sites) and on studies reporting quantitative uncertainty metrics. The search is performed primarily in ScienceDirect, ResearchGate, MDPI, Energies and Wind Energy Science, with combinations of following keywords: “wind measurement”, “wind profiling”, “onshore wind”, “complex terrain”, “mountainous”, “forest”, “profiling lidar”, “Doppler lidar”, “UAV”, “drone-based wind measurement”, “uncertainty”, “bias”, “error”, “flow model”, “WAsP”, “CFD”. Studies are included if they:

(i) addressed onshore wind measurement and linear flow models in mountainous, hilly, and forested terrain.
(ii) reported the measurement uncertainty of wind speed and direction, for vertical profiling LiDAR or fixed-wing UAVs.

https://doi.org/10.5194/wes-2026-92
Preprint. Discussion started: 18 June 2026

(iii) reported the model's uncertainty of wind speed for spatial extrapolation, using single-point measurement data as input.

(iv) covered publications from approximately 2010 onwards, at global scale.

Additional relevant references are identified through backward and forward citation tracking of key papers. Where no suitable data were available for complex terrain, the search is cautiously extended to studies in gentle terrain to provide indicative benchmarks. This step is to document realistic ranges for uncertainty components of both technologies, ensuring that the subsequent quantitative models are grounded in state-of-the-art knowledge.

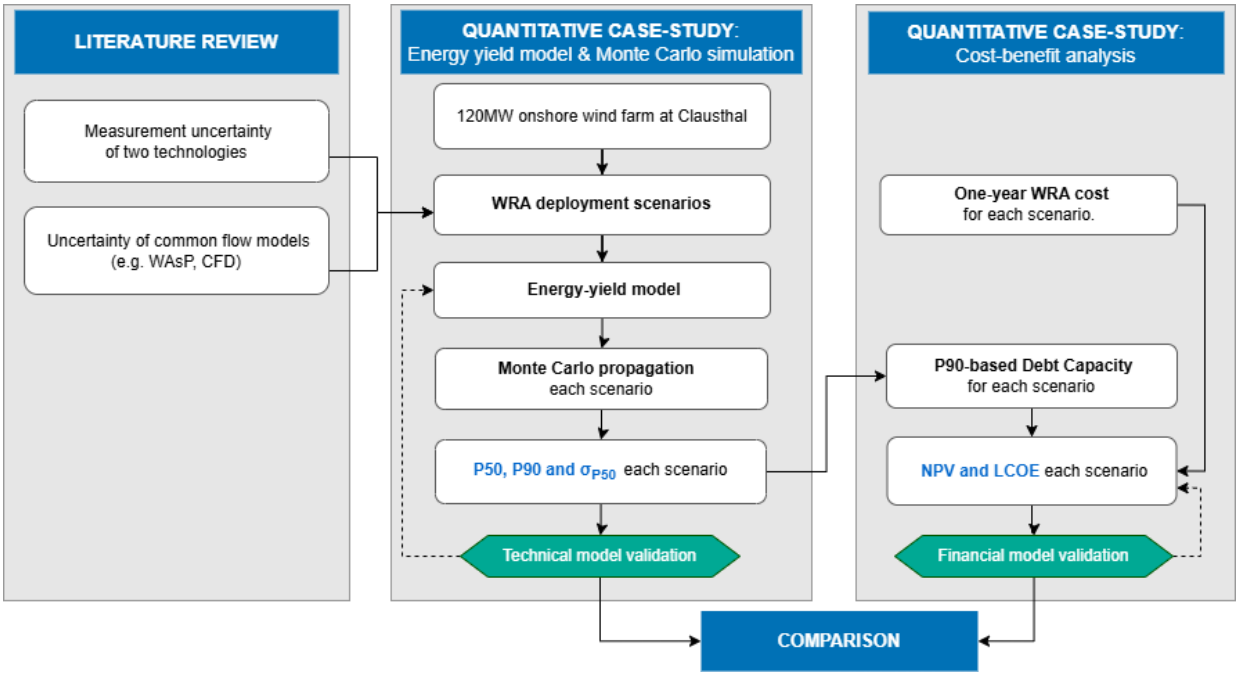

Figure 1: Overall methodological framework of the thesis (solid arrows indicate the primary sequence of modelling and analysis steps; dashed arrows indicate validation links between components)

2. 2 Quantitative case study

The quantitative case study is carried out for a hypothetical 20-turbine onshore wind farm in complex terrain at Clausthal-Zellerfeld, Harz Mountains, Germany. Case-study research is well suited to complex, context-dependent systems (Annamalah, 2024), allowing a detailed exploration of WRA in non-uniform terrain where flow and access are highly site specific.

Energy yield model:

In this case study, an energy yield model using Python is built for a 120 MW wind farm, driven by an existing one-year WindCube LiDAR dataset at 160 m above ground (Rausch et al., 2022) in Clausthal. The site consists of forested upland

https://doi.org/10.5194/wes-2026-92
Preprint. Discussion started: 18 June 2026

eawe european academy of wind energy
Open Access WIND ENERGY SCIENCE DISCUSSIONS

plateau (390-821 m a.s.l.) with strong vertical shear and directional veer (Bretschneider et al., 2021; Rausch et al., 2022). The terrain was assessed per IEC 61400-1:2019 using the Terrain Slope Index (TSI) and Terrain Variation Index (TVI) over three assessment radii (5z_hub, 10z_hub, 20z_hub) for all 20 turbine locations (IEC, 2019). TSI_{30} values remain consistently low across all radii (mean 1.66°, maximum 6.22°), confirming negligible orographic steepness. TVI_{30} values, however, reveal pronounced short-range terrain heterogeneity (mean 2.89%, maximum 7.7% at 5z_hub), indicative of localised flow separation and non-standard wind shear. Applying the IEC worst-case classification rule, the site exceeds the Simple category threshold. On a site-average basis, 80% of turbines fall within the Simple-to-Low complexity range; accordingly, the site is treated as Low-complexity terrain with flow-distorting conditions throughout this study.

A V162-6.2 MW turbine is selected to match the local wind climate (see Figure 2). The power curve and detailed configuration of the V162-6.2 MW can be found in (Zagubień et al., 2024).

The 10-min measured wind speed ($U_{ms,}$) and direction recorded at a reference height (Rausch et al., 2022) are binned into 12 directional sectors (e.g. Figure 2.a) and treated as the reference ("truth") at the measurement point. Wind conditions at each turbine are then derived using a WAsP-type framework: vertical and horizontal extrapolation via a sector-wise speed-up factor $\mathbf{F(\theta, ms, t)}$ incorporating orography, roughness and obstacle effects, as in Eq.(1) (Kamdar et al., 2021). These effects are extracted from GLO-30 digital elevation map (DEM) (OpenTopography, 2021) and global landcover map (Zanaga et al., 2021). The translated series of wind speed U_t at each turbine is also treated as the modelled reference.

$$U_t(\theta) = U_{ms}(\theta) \times F(\theta, ms, t) \quad (1)$$

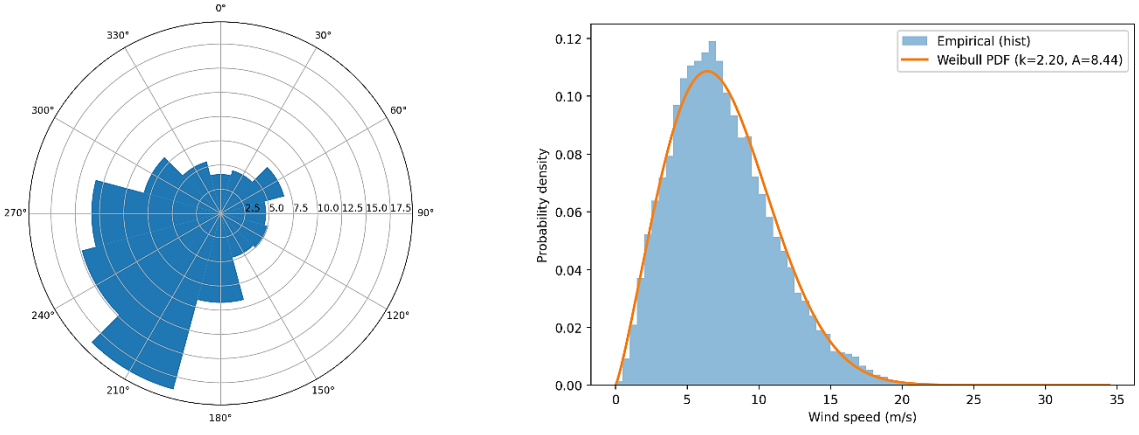

(a) Wind rose (b) Weibull distribution

Figure 2: Wind climate at Clausthal's measured site

For each turbine and sector, a two-parameter Weibull distribution is fitted to the hub-height series and combined with the manufacturer's power curve to compute gross AEP, followed by standard-loss factors (wake, availability, electrical, curtailment) (Afanasyeva et al., 2016; Kamdar et al., 2021; Schaffarczyk, 2014). This model provides the basic for validating

https://doi.org/10.5194/wes-2026-92
Preprint. Discussion started: 18 June 2026

different UAV- and LiDAR-based deployments at site. The deployment designing logic is driven by farm size and features of measurement approaches. Four deployment scenarios (see Figure 3) are defined:

- Scenario 1 (LiDAR_1) uses a single vertical profiling LiDAR at the measurement point and relies on flow model to estimate the turbines' wind speed.
- Scenario 2 (LiDAR_2) employs two vertical profiling LiDARs, one as in Scenario 1 and a second on the opposite side of the farm. Every turbine lies within 4 km of both LiDARs, enabling cross-validation between the two measured datasets and reduces flow model error as well as uncertainty, as recommendation at (Menke et al., 2020).
- Scenario 3 (UAV_2) is designed to minimise the number of drones used. The flight path design is selected to achieve the standard 10-minute resolution across the farm. The study adopts the features and improvements of the Alveo AB fixed-wing UAV system (Hassani, 2023), including a recommended endurance of ~5 hours under normal conditions, an average airspeed 24-25 m/s, and maximum speed 39-40 m/s. A single drone continuously surveys the site along a 14.5 km circuit, passing directly over 13 turbine locations, while the second unit remains on charge. Wind conditions at the remaining 7 turbines are derived from the flow model.
- Scenario 4 (UAV_4) focuses on directly measuring at 20 turbine locations through two drones that map the site simultaneously along the proposed paths, while two additional drones are charging or in reserve. Therefore, the scenario removes the reliance on a flow model.

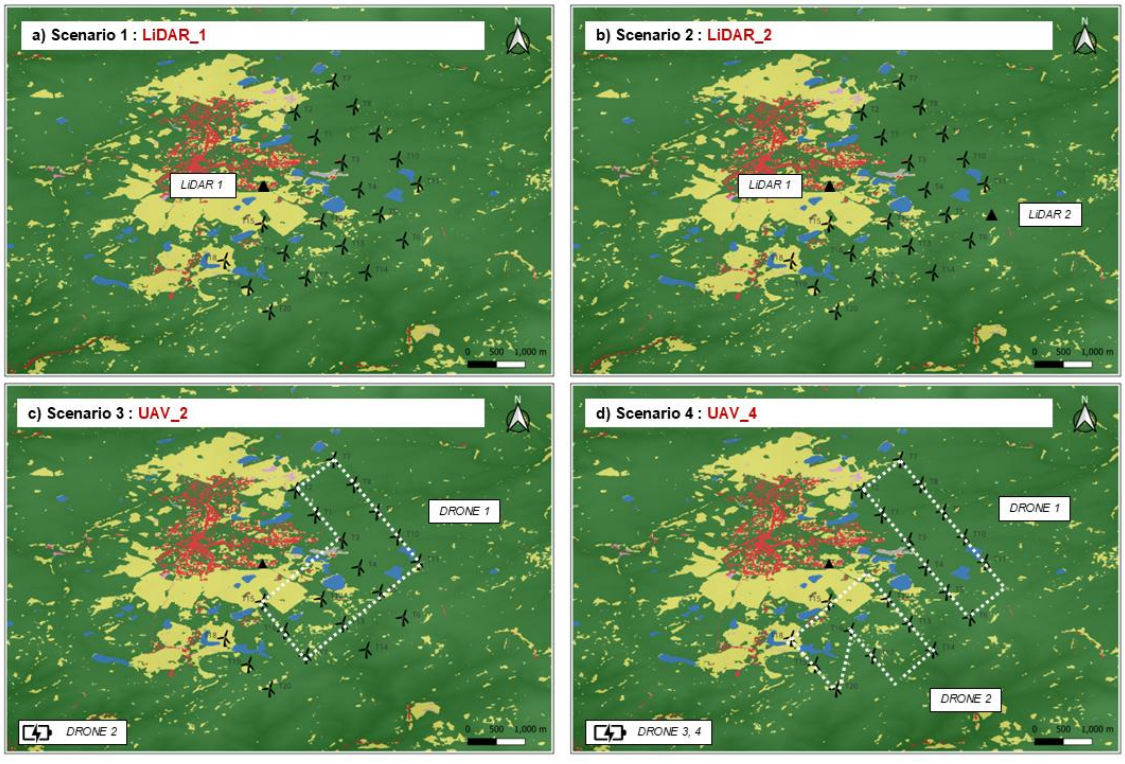

Figure 3: Illustration of four deployment scenarios

https://doi.org/10.5194/wes-2026-92
Preprint. Discussion started: 18 June 2026

eawe european academy of wind energy
Open Access WIND ENERGY SCIENCE DISCUSSIONS

Uncertainty definitions and Monte Carlo set-up:

Three uncertainty components are represented explicitly in the Monte Carlo framework:

- Measurement wind-speed uncertainty $\varepsilon_{WS} \sim \mathcal{N}(0, \sigma_{ws}^2)$ is applied as an additive error to the 10-min wind-speed series. Standard deviation σ_{ws} (m/s) refers to instrumental uncertainty and short-term variability. $\sigma_{ws} > 0$.
- Measurement wind-direction uncertainty $\varepsilon_{WD} \sim \mathcal{N}(0, \sigma_{wd}^2)$ is applied as an additive error to the 10-min wind-direction series. Standard deviation σ_{wd} (°) captures heading-sensor uncertainty.
- Flow-model (spatial-extrapolation) uncertainty $F_{flow} \sim \mathcal{N}(1, \sigma_{flow}^2)$ is applied as a multiplicative factor to sector-wise speed-up $F(\theta, ms, t)$ per turbine. Standard deviation σ_{flow} (%) reflects the combined effect of terrain and model-structure uncertainty to the translated wind speed. $F_{flow} > 0$.

Here, σ_{ws}, σ_{wd} and σ_{flow} are scenario-dependent and taken from the literature review. This allows measurement and flow-model uncertainties to be treated as coupled, reflecting the fact that the flow model uses measured data as input. The Monte Carlo engine is used to propagate these uncertainties through the energy-yield model. For each scenario, $N = 5000$ simulations are run. In each run, the wind field is perturbed by sampling ε_{WS}, ε_{WD} and F_{flow}, and the full energy-yield pipeline is executed. The outputs include the AEP estimation, which is expressed by the simulated P50 and P90 values (MWh), and the standard deviation of P50, $\sigma(P_{50})$ (MWh, %). Monte Carlo simulation is chosen, following prior work (e.g. (Afanasyeva et al., 2016; Gleim et al., 2018; Kwon, 2010)), because it (i) treats AEP as a full probability distribution rather than collapsing uncertainty into a single "square-root-of-sum-of-squares" value, and (ii) can represent dependence between uncertainty sources explicitly.

Cost-benefit analysis

To link the technical results to investment relevance, a cost-benefit analysis is carried out. Although WRA campaign commonly accounts for <2% of onshore project's capital expenditure (CAPEX) (IEA Wind Task 36, 2022), not every campaign results in a project progressing to investment or construction, so these costs remain a critical factor in developers' decision-making (Clifton et al., 2016). One-year WRA campaign cost is estimated for four scenarios in this work, which normally includes: rental, deployment and commissioning, calibration, operations/maintenance, and data processing.

Vertical profiling LiDARs are mature commercial products, so in the LIDAR_1 and LIDAR_2 scenarios, costs are estimated from commercial rental rates sourced from public quotations and combined with installation, power, and scheduled maintenance allowances. By contrast, UAV systems for wind measurement have less transparent market pricing. In the UAV_2 and UAV_4 scenarios, costs are built bottom-up, with capital expenditure CAPEX (drones, control system, charging equipment and container) and operational expenditure OPEX (routine maintenance, staff and field logistics) itemised separately. A profit margin is added to reflect the service provision and to ensure like-for-like comparability with LiDAR rental quotes, which already include vendor margins. This approach follows a standard cost-plus pricing methodology, detailing in (Amaral & Guerreiro, 2018; Oh & Son, 2019).

https://doi.org/10.5194/wes-2026-92
Preprint. Discussion started: 18 June 2026

On the benefit side, the analysis focuses on debt capacity, modelled via a P90-based Debt Service Coverage Ratio (DSCR) constraint (Henderson et al., 2014; Mora et al., 2019) in a 25-year project-finance model, which determines as the maximum amount of project-finance debt a wind project can support given lenders' requirements. This study assumes a DSCR target of 1.35 for onshore projects in complex terrain (Clausthal), following (Henderson et al., 2014). The DSCR-based debt capacity feeds into a standard project cash flow model to evaluate NPV and LCOE. NPV is defined here as the present value of equity cash flows minus the initial equity investment, as in Eq.(2). LCOE is defined as the ratio of the discounted sum of all project costs to the discounted sum of net energy production (Mora et al., 2019), as in Eq.(3).

$$\mathrm{NPV} = \sum_{i=1}^{25} \frac{\mathrm{EBIT_i}(1-\mathrm{Tax})}{(1+\mathrm{WACC})^i} - \mathrm{CAPEX} = \sum_{i=1}^{25} \frac{(\mathrm{P90_i} \times \mathrm{Tariff_i} - \mathrm{OPEX_i})(1-\mathrm{Tax})}{(1+\mathrm{WACC})^i} - \mathrm{CAPEX} \quad (2)$$

$$\mathrm{LCOE} = \frac{\mathrm{CAPEX} + \sum_{i=i}^{25} \frac{\mathrm{OPEX_i}}{(1+\mathrm{WACC})^i}}{\sum_{t=i}^{25} \frac{\mathrm{P90_i}}{(1+\mathrm{WACC})^i}} \quad (3)$$

where, $\mathbf{EBIT_i}$ is the earnings before interest and tax in year i; $WACC$ is the weighted average cost of capital; $\mathrm{Tariff_i}$ is the realised average power price (€/MWh); $\mathrm{OPEX_i}$ is operating expenditure (fixed and variable, €) in year i; CAPEX is the project's capital expenditure (€).

The following financial inputs are used:

- Investment cost (CAPEX): 1,600 €/kW of installed capacity (Christoph et al., 2024)
- Fixed operational cost (fix-OPEX): 32 €/year/kW of installed capacity (Christoph et al., 2024)
- Variable operational cost (var-OPEX): 0.007 €/kWh (Christoph et al., 2024)
- Electricity selling price: feed-in-tariff of 6.54 ct/kWh (Christoph et al., 2024; Reuters, 2024), applying for 25 years
- Debt condition:
  - DSCR target: 1.35 (Henderson et al., 2014)
  - Cost of debt: 5.5% (Christoph et al., 2024)
  - Time: 15 years (assumption)
  - Tax: 20% (assumption)

2.3 Sensitivity analysis

The sensitivity analysis focuses on two scenario-specific uncertainty inputs: the measurement-uncertainty σ_{ws}, and the flow model uncertainty σ_{flow}. Each input is independently perturbed by ±2% points around their chosen scenario-specific values. This tests how sensitive the output metrics P50, P90, NPV, and LCOE are to plausible variations in the assumed uncertainty levels. The ±2% point perturbation was chosen because it falls within the spread of uncertainty values chosen for the Monte Carlo simulations in this study, as synthetised in Section 3.2.

https://doi.org/10.5194/wes-2026-92
Preprint. Discussion started: 18 June 2026

eawe european academy of wind energy
Open Access WIND ENERGY SCIENCE DISCUSSIONS

3 Results

3.1 Measurement and spatial modelling uncertainties from literature review

The literature review confirms that both vertical profiling LiDARs and fixed-wing UAVs can achieve comparable point-measurement accuracy when appropriately processed. According to (Bischoff et al., 2024; Kim et al., 2016), in complex terrain, profiling LiDARs typically show mean wind-speed biases of about -0.3m/s to +0.5 m/s (-4% to +6%), standard uncertainties around ±0.2-0.5m/s when benchmarked against mast references. Wind-direction uncertainties are roughly 4-7° (Kim et al., 2016; Knoop et al., 2021).

Fixed-wing UAVs, such as the MASC platform, demonstrate negligible mean bias, while uncertainties of the order ±0.5 m/s in complex escarpment terrain (Wildmann et al., 2014, 2017). While in more gentle terrain, the system reaches 10-min wind-speed uncertainty of ~0.1m/s and direction fluctuation of ~10° to mast references (Boventer et al., 2024).

The linear spatial-modelling uncertainty, such as WAsP model, is generally 5% in suitable conditions, and exceed 8-9.5% in highly rugged sites (Dörenkämper et al., 2020; Indasi et al., 2016; Sheehan et al., 2022). CFD models, including RANS and LES approaches, generally achieve mean wind speed errors within 10-20% in complex terrain, with standard deviations often in the range of 1-2m/s (Bechmann et al., 2011; Fernando et al., 2019).

3.2 Chosen uncertainty-values for deployment scenarios

The uncertainty values adopted for the Clausthal case study are derived from observations of the aforementioned validation studies and are intended to represent typical performance for 10-minute mean wind statistics. The specific combination of uncertainty components for each deployment scenario is summarized in Table 1.

For LiDAR's scenarios, a wind speed uncertainty of ±0.4 m/s (~5 % of the long-term mean wind speed at Clausthal) and a direction uncertainty of 7° are used. These values lie in the mid-range of those reported by (Kim et al., 2016), (Bischoff et al., 2024) and (Knoop et al., 2021). Regarding flow-model uncertainty, an 8% standard uncertainty in wind speed due to the flow model is assigned to Scenario LiDAR_1. This value is deliberately chosen near the upper end of the WAsP uncertainty range for complex terrain (Indasi et al., 2016) and reflects that the flow field is constrained by only one profiling LiDAR, so the linear model retains a relatively high degree of structural uncertainty. In Scenario LIDAR_2, the presence of a second LiDAR enables cross-checking of the spatial speed-up pattern and partial calibration of the linear model between two measurement points, so 5% uncertainty reflects the "suitable conditions" as reported in (Sheehan et al., 2022).

For fixed-wing UAV measurements, a wind speed uncertainty of ±0.5 m/s (~6.5 % of Clausthal's mean wind speed) and a direction uncertainty of 10° are assumed, based on reports by (Wildmann et al., 2014, 2017) and (Boventer et al., 2024). In terms of flow-model uncertainty, for UAV_2, a 5% flow-model uncertainty is applied only to the seven turbines without direct UAV measurements. The dense UAV sampling reduces the model's role to interpolating between multiple well-distributed measurement points, again bringing the extrapolation problem closer to a "well-characterised" case as reported in (Sheehan et

https://doi.org/10.5194/wes-2026-92
Preprint. Discussion started: 18 June 2026

eawe european academy of wind energy
Open Access WIND ENERGY SCIENCE DISCUSSIONS

al., 2022). Finally, in Scenario UAV_4, each turbine is directly sampled by UAV flights, and no additional flow model uncertainty is applied.

Table 1: Scenario-specific uncertainty inputs

Scenario	**LiDAR_1** (base case)	**LiDAR_2**	**UAV_2**	**UAV_4**
1. Measurement uncertainty ▪ Wind speed (ε_{WS}) ▪ Wind direction (ε_{WD})	σ_{ws} = ±0.4 m/s σ_{wd} = ±7°	σ_{ws} = ±0.4 m/s σ_{wd} = ±7°	σ_{ws} = ±0.5 m/s σ_{wd} = ±10°	σ_{ws} = ±0.5 m/s σ_{wd} = ±10°
2. Flow-model uncertainty ▪ Wind speed (F_{flow}) ▪ Noted:	σ_{flow} = ±8% *apply to all turbines*	σ_{flow} = ±5% *apply to all turbines*	σ_{flow} = ±5% *apply to 7 turbines*	*non-apply*

3.3 Techno-economic comparison

Table 2 reports the Monte Carlo results for the energy yield metrics of four scenarios and their corresponding economic outcomes.

Table 2: Summary of techno-economic comparison results

Scenario	**LiDAR_1** (base case)	**LiDAR_2**	**UAV_2**	**UAV_4**
AEP UNCERTAINTY				
Mean AEP (P50) [MWh]	468,893	470,761	471,390	472,423
P50's standard deviation [MWh, %]	8,916	5,515	2,385	92
	1.90%	1.17%	0.51%	0.02%
P90 [MWh]	457,106	463,536	468,141	472,303
P90/P50 ratio [%]	97.49%	98.47%	99.31%	99.97%
PROJECT FINANCIAL INDICATORS AND NPV				
Share of Debt [% CAPEX]	88.5%	90.0%	91.0%	91.9%
WACC [%]	4.7%	4.7%	4.6%	4.6%
P90-Revenue [€]	747,368,892	757,881,029	765,410,308	772,216,206
NPV [€]	73,655,594	79,208,524	83,063,816	86,765,322
NORMALIZING NPV GAINS BY €1 OF EXTRA WRA COST				
ΔNPV/ΔWRA	-	76.5	186.3	101.0
LCOE				
LCOE [€/MWh]	44.31	43.66	43.23	42.82

AEP uncertainties:

Across LiDAR_1 → LiDAR_2 → UAV_2 → UAV_4, the median of the Net AEP distribution, P50, increases gradually. The base case LiDAR_1 exhibits the lowest P50 (468,893 MWh). Relative to LiDAR_1, annual gains are roughly +0.4% for LiDAR_2, +0.5% for UAV_2, and +0.8% for UAV_4 (Figure 4.a). The standard deviation of P50 (σ_{P50}), which reflects the dispersion of the Net AEP distribution, decreases much more strongly than P50 increases. Expressed as a percentage of P50, σ_{P50} shrinks sharply from 1.90% in LiDAR_1 to 1.17% in LiDAR_2, 0.50% in UAV_2, and just 0.02% in UAV_4 (Figure

https://doi.org/10.5194/wes-2026-92
Preprint. Discussion started: 18 June 2026

eawe european academy of wind energy
Open Access WIND ENERGY SCIENCE DISCUSSIONS

4.b). Overall, the primary effect of enhanced deployment is therefore not a large upward shift in expected energy, but a substantial tightening of the AEP distribution.

P90 is another key metric, it not only reflects the lower-tail of the AEP distribution but also directly feeds DSCR-based debt sizing. Across the deployment scenarios, P90 increases monotonically relative to the base case LiDAR_1, with percentage uplifts (ΔP90) of +1.4%, +2.4%, and +3.3% for LiDAR_2, UAV_2, and UAV_4, respectively (Figure 5). Consistently, the P90/P50 ratio rises from 97.49% to 99.97%, indicating reduced downside risk and increasingly narrow uncertainty bands.

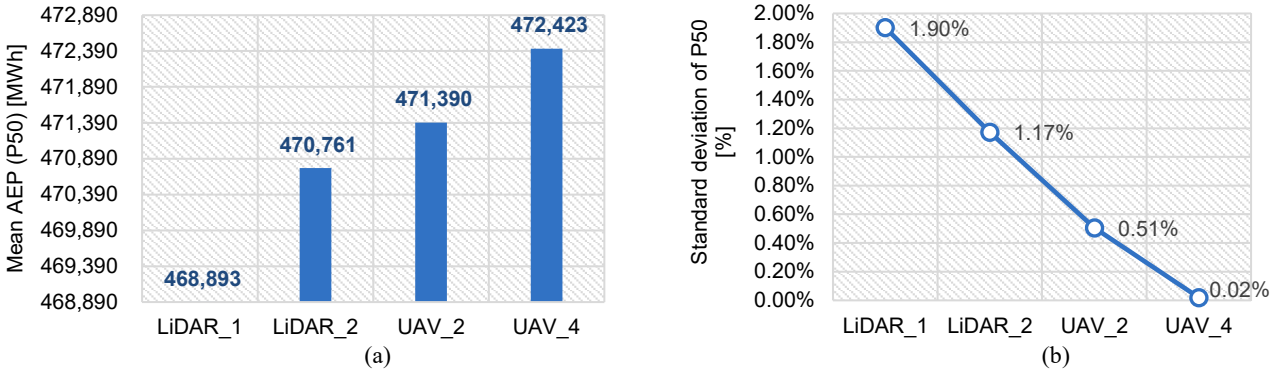

Figure 4: Annual P50 metric by deployment scenarios:
(a) P50 improvement compared to the base case; (b) P50's standard deviations (σ_{P50})

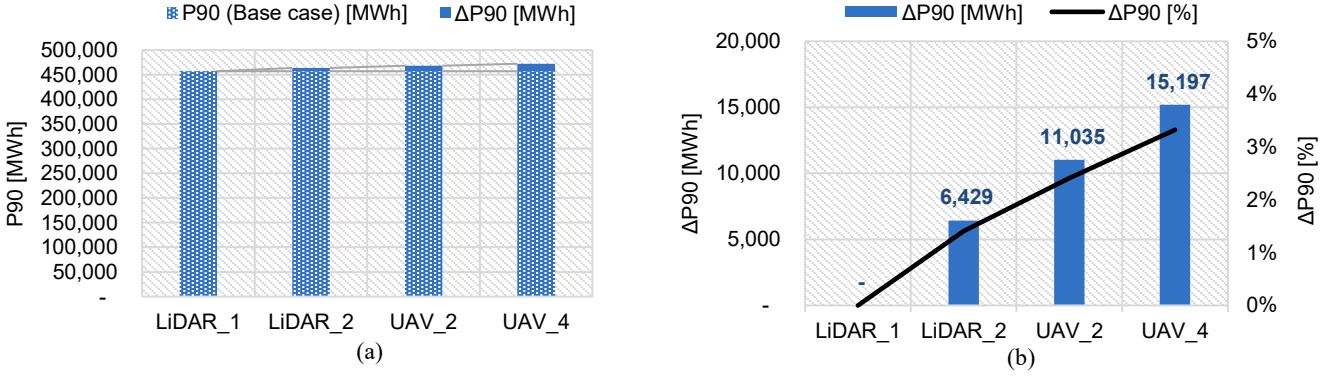

Figure 5: Annual P90 metric by deployment scenarios:
(a) P90 and ΔP90 improvement compared to the base case; (b) Zoom-in of ΔP90 improvement

As the differences between the measurement uncertainties of the two technologies are modest, these patterns reflect that the main gain from the additional LiDAR and UAVs is not sharper point-measurement accuracy, but reduced flow model uncertainty through improved spatial coverage. In other words, additional devices enhance spatial extrapolation robustness rather than instrument precision.

https://doi.org/10.5194/wes-2026-92
Preprint. Discussion started: 18 June 2026

eawe european academy of wind energy
Open Access WIND ENERGY SCIENCE DISCUSSIONS

For validation, the comparison is restricted to the base case, for which similar methodological approaches are available in the literature. LiDAR_1' Monte Carlo results with a farm-scale AEP standard deviation of about 1.9% of P50, aligns with (Gleim et al., 2018). While the average turbine-level AEP standard deviation is ~8%, consistent with published uncertainty stacks for single turbines (Kwon, 2010). This supports the plausibility of the uncertainty framework used.

Cost-benefit analysis

One-year WRA campaign costs are estimated with the range from approximately 75.6 k€ in LiDAR_1 to 148.2 k€ in LiDAR_2, 126.8 k€ in UAV_2 and 205.3 k€ in UAV_4 (Figure 6). Relative to the LiDAR_1 campaign cost, LiDAR_2 increases cost by ~96%, UAV_2 shows an estimated 68% increase, while UAV_4 is projected to have a significantly greater rise of approximately 172%. Nevertheless, UAV_2 remains slightly more affordable than the LiDAR_2 campaign, at approximately 15% lower cost.

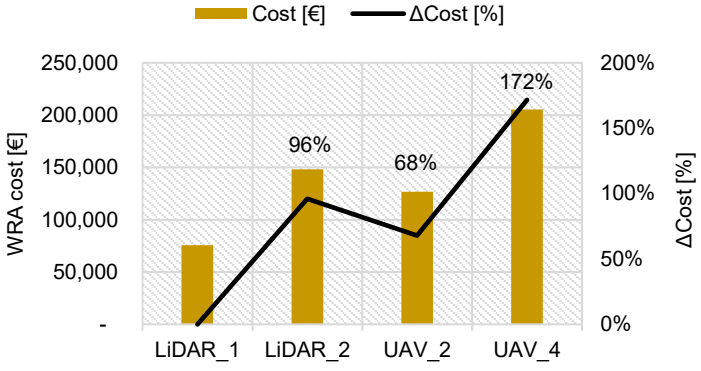

Figure 6: One-year WRA cost estimation across deployment scenarios, and Cost increases compared to the base case (LIDAR_1).

As P90 increases across the scenarios, the P90-based DSCR model permits a higher debt share in CAPEX, also P90-based revenues rise, thereby affecting both NPV and LCOE.

Specifically, adding one additional LiDAR (LiDAR_2) increases P90 by 1.4% compared with LiDAR_1. Although the resulting reduction in WACC is small (Table 2), the combination of higher P90-based revenue and slightly improved financing conditions leads to a 7.5% increase in NPV (+€5.77 M€) (Figure 7). The UAV scenarios follow the same qualitative pattern. Improvements in P90 translate into NPVs of approximately €83.1 M (+12.8%) for UAV_2 and €86.7 M (+17.8%) for UAV_4, respectively.

In contrast, LCOE declines as deployment intensity increases. Starting from €44.31/MWh for LiDAR_1, LCOE decreases to €43.66/MWh for LiDAR_2, €43.23/MWh for UAV_2, and €42.82/MWh for UAV_4. The largest reduction, 3.5%, occurs between UAV_4 and the base case (Figure 8). These reductions reflect the combined effect of higher expected net energy (P50 and P90) and slightly cheaper capital. The resulting LCOEs lie in the lower half of recent German onshore ranges (4.3-9.2 €cents/kWh) (Christoph et al., 2024), supporting the plausibility of the financial assumptions.

https://doi.org/10.5194/wes-2026-92
Preprint. Discussion started: 18 June 2026

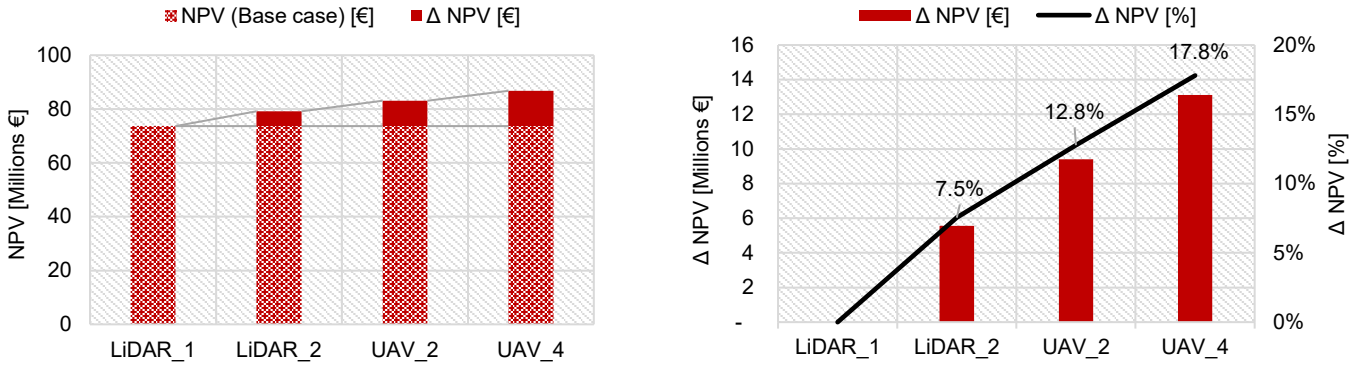

(a) (b)

Figure 7: Project NPV by deployment scenarios:
(a) NPV and ΔNPV improvement compared to the base case; (b) Zoom-in of ΔNPV improvement

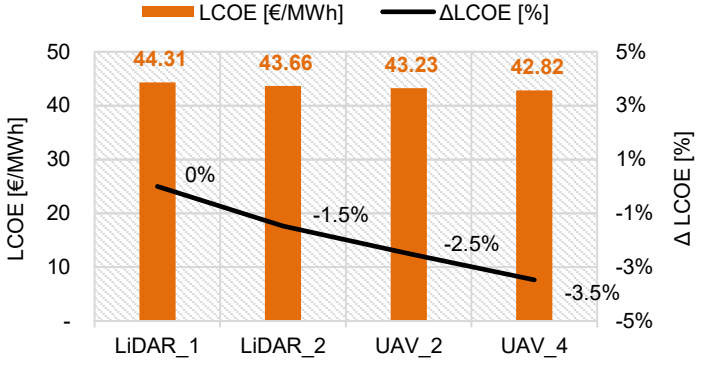

Figure 8: LCOE and ΔLCOE reduce compared to the base case

Under the cost-benefit perspective, the incremental net present value per additional euro of WRA spend (ΔNPV/ΔWRA) provides a compact measure of the economic efficiency of each deployment option. Normalising NPV gains by €1 of extra WRA cost gives approximately ~76, 184 and 101 €/per€ for LiDAR_2, UAV_2 and UAV_4, respectively. All enhanced scenarios are value-creating relative to LiDAR_1. Among scenarios, UAV_2 offers the strongest return, capturing most of the AEP and financing benefits from improved spatial coverage at moderate additional cost.

3.4 Sensitivity analysis

Figure 9-10 show how the key project indicators respond to a ±2% point change in two uncertainty inputs: wind-speed measurement uncertainty and flow-model uncertainty. Grey bars represent a negative impact on project indicators (i.e. lower P50, P90, and NPV, or higher LCOE) resulting from the input change, while coloured bars represent a positive impact. For

https://doi.org/10.5194/wes-2026-92
Preprint. Discussion started: 18 June 2026

eawe european academy of wind energy
Open Access WIND ENERGY SCIENCE DISCUSSIONS

each bar, the bottom axis reports the relative change in %, and the text on the bars gives the corresponding absolute variation in MWh, M€, or €/MWh.

When wind speed measurement uncertainty changes ±2%, with fixed flow model uncertainty, the impact on P50 and P90 of all four scenarios remains below 0.3% (Figure 9). Whereas an equivalent change in flow-model uncertainty, with the measurement term held fixed, shifts the entire AEP distribution more noticeably. P50 and especially P90 values for LIDAR_1, LIDAR 2 and UAV_2 vary more strongly, by roughly 0.4% for P50 and 1% for P90 (Figure 10). However, these values for UAV_4 remain unchanged (Figure 10). These show that in the total uncertainty "budget", the wind speed measurement component contributes only a relatively small fraction compared with the flow model component. These findings are consistent with the comprehensive review by (Barber et al., 2022).

An asymmetric response is also observed. The increase +2% of the uncertainty reduces P50 and P90 more strongly than the gains obtained from a −2% reduction (both Figure 9 and Figure 10). This behavior is consistent with the models' logic, as P50 and especially P90 are decreasing functions of AEP deviation. Moreover, the asymmetry is stronger for measurement uncertainty. When this term is reduced by 2%, its standard deviation becomes very small, and the Monte Carlo spread nearly collapses. In contrast, flow-model uncertainty remains relatively large even after a 2% reduction. This indicates that reducing flow-model uncertainty offers greater potential for improving yield estimates than minimising measurement uncertainty alone.

Across the scenarios, the sensitivity levels of the two LiDAR scenarios clearly demonstrate the dominant impacts of flow model uncertainty and the asymmetry pattern. Their P90s are also the most sensitive to flow model fluctuations. The sensitivity level of UAV_2 is particularly interesting because it exhibits a different pattern from the other scenarios: the response is much less asymmetric. This is because measurement uncertainty is applied to all turbines, while flow-model uncertainty affects only part of the farm. When aggregated, these effects balance each other more evenly.

The P90/P50 ratio further contextualises these findings. It remains insensitive to ±2% measurement uncertainty across all scenarios. In contrast, flow-model uncertainty compresses the P90/P50 ratio more noticeably for LiDAR-based scenarios ($\Delta \approx \pm 0.01$), while Scenario 4 exhibits near-zero sensitivity to both sources.

At the economic level, the three groups of input parameter changes show very different degrees of "leverage" on NPV and LCOE. When the wind measurement uncertainty changes by ±2% (Figure 9), both NPV and LCOE change only slightly. This, again, demonstrates that small changes in measurement uncertainty only slightly shift the AEP distribution, so the NPV and LCOE are barely affected. In contrast, when the flow model uncertainty changes by ±2% (Figure 10), NPV reacts much more strongly, and LCOE is also more sensitive than in the wind measurement case.

https://doi.org/10.5194/wes-2026-92
Preprint. Discussion started: 18 June 2026

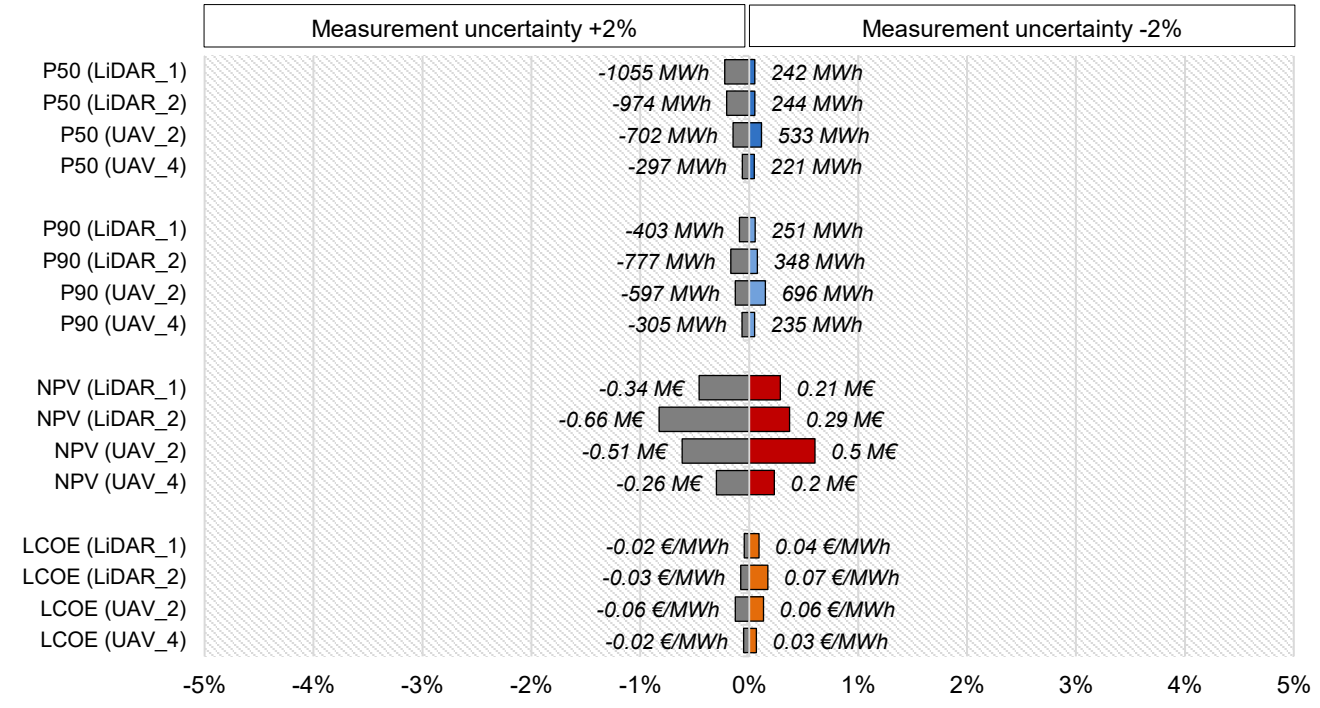

Figure 9: Sensitivity of P50, P90, NPV and LCOE to ±2% measurement uncertainty in wind speed, by deployment scenarios

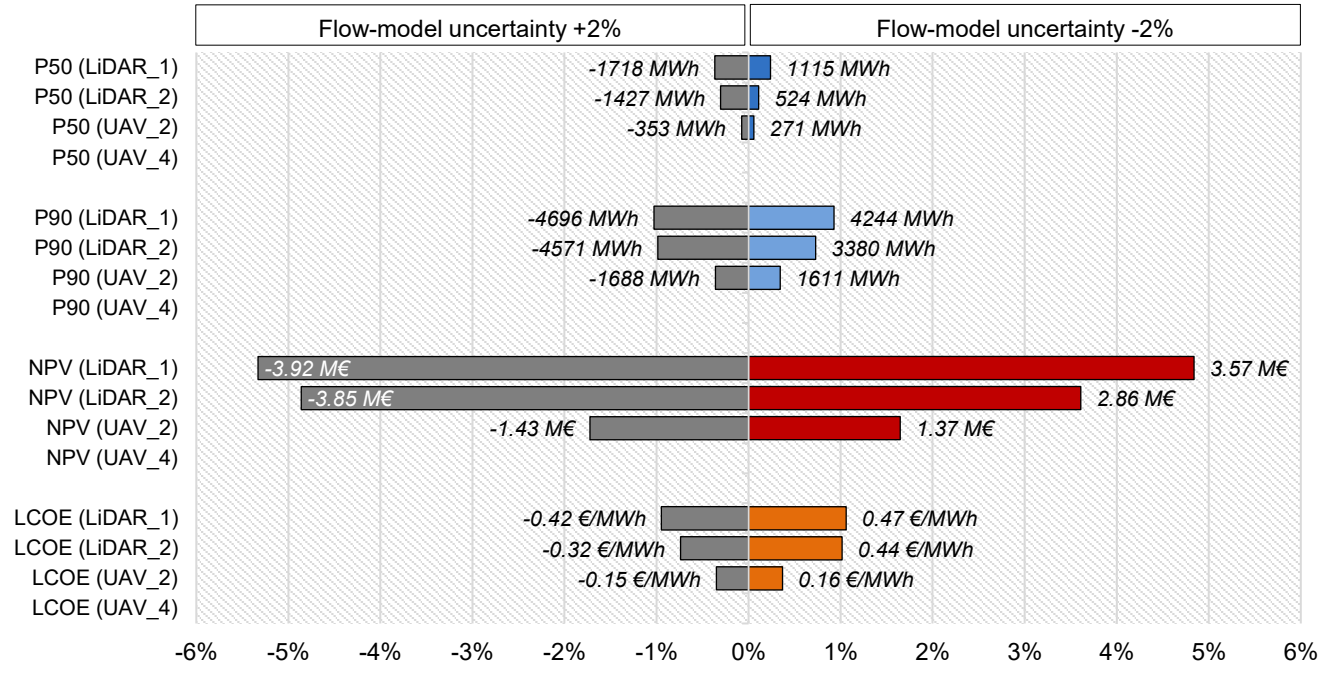

Figure 10: Sensitivity of P50, P90, NPV and LCOE to ±2% flow-model uncertainty in wind speed by deployment scenarios

https://doi.org/10.5194/wes-2026-92
Preprint. Discussion started: 18 June 2026

eawe european academy of wind energy
Open Access WIND ENERGY SCIENCE DISCUSSIONS

4. Discussion

Several methodological limitations restrict the external validity of these findings. First, the comparison is not based on a side-by-side field experiment: LiDAR data from Clausthal are combined with literature-based uncertainty parameters from different sites, set-ups and processing methods. Therefore, the results rely on conservative assumptions. Second, the energy-yield model uses a simplified WAsP-type flow framework and an assumed reduction in flow-model uncertainty (8% → 5%) based on literature reviews, that has not been experimentally verified. AEP uncertainty, thus, remains approximate. Third, the uncertainty analysis focuses only on random wind-speed and wind-direction components linked to LiDAR and UAVs, excluding other key sources (e.g. long-term correction, interannual variability, wake and power-curve uncertainty), making the very low residual uncertainty in UAV_4 optimistic.

Moreover, the cost-benefit analysis is based on illustrative campaign costs with estimated expenditure components for a specific project and a simplified feed-in-tariff-based finance model, without detailed subsidies, power purchase agreements (PPAs), or merchant price risk. Finally, non-monetised benefits and practical considerations that may strongly influence technology choice are not quantified in this work. The conclusions are therefore directional and comparative, not universal.

5. Conclusion

The study systematically compares vertical profiling LiDAR and fixed-wing UAV deployments for WRA in flow-distorting, low complexity terrain, linking measurement and flow model uncertainties to AEP distributions and financial metrics for a representative onshore farm at Clausthal, Germany. The literature review shows that once systematic biases are calibrated, residual random measurement uncertainties at this site for both technologies cluster around ±0.4-0.5m/s and ±7–10°.

The energy-yield modelling and cost-benefit analysis highlight the advantages of the UAV configurations in the wind measurement. Across the four deployment scenarios, **LiDAR_1 → LiDAR_2 → UAV_2 → UAV_4**, the median P50 increases slightly while P90 improves by 1.4-3.3%, reflecting a progressive narrowing of the AEP uncertainty distribution. the P90/P50 ratio approaches unity, indicating a progressively tighter and more bankable yield estimate. These improvements translate into NPV gains of up to ~18% and LCOE reductions of ~3.5% relative to the LiDAR_1 (Base case).

Taken together, the results answer well the research question. For the Clausthal case, the techno-economic advantage of UAV-based deployments over vertical profiling LiDAR lies less in superior sensor accuracy and more in reducing reliance on flow models through improved direct spatial coverage. This is reinforced by the sensitivity analysis, in which LIDAR-based scenarios show substantially greater exposure to flow-model perturbations in both AEP and financial metrics.

For other onshore projects in flow-distorting terrain, however, measurement and extrapolation strategies that work well at one site may perform very differently at another. The flexibility of fixed-wing UAV deployments can offer a structural advantage for tailoring WRA campaigns. The implication is not that UAVs universally outperform vertical profiling LiDARs, but in moderate-to-high complex terrain, repositionable instruments that directly capture spatial variability provide a more robust basis for AEP estimation and investment decisions.

https://doi.org/10.5194/wes-2026-92
Preprint. Discussion started: 18 June 2026

Data availability

The Python model and Excel-based financial model in this study are available on GitHub (DOI:10.5281/zenodo.20346846).

Declaration of generative AI

During the preparation of this work, the authors use ChatGPT (OpenAI) to improve scientific writing and to support energy yield model development, specifically for cross-checking Python code logic and resolving errors. All outputs were independently reviewed and validated by the authors. The authors take full responsibility for the content of this study.

Author contributions

PAN: Conceptualization, Methodology, Formal Analysis, Writing – original draft preparation.
EV: Methodology, Writing – Review & editing.
DH: Conceptualization, Review & editing.

Competing interests

D.H. is the founder of Alveo AB, which is commercially developing the UAV platform mentioned in this study, and provided the technical data used in designing four measurement scenarios. The remaining authors declare no competing interests.

References

Afanasyeva, S., Saari, J., Kalkofen, M., Partanen, J., & Pyrhönen, O. (2016). Technical, economic and uncertainty modelling of a wind farm project. *Energy Conversion and Management*, *107*, 22–33. https://doi.org/10.1016/j.enconman.2015.09.048

Alaoui-Sosse, S., Durand, P., Medina, P., Pastor, P., Gavart, M., & Pizziol, S. (2022). BOREAL—A Fixed-Wing Unmanned Aerial System for the Measurement of Wind and Turbulence in the Atmospheric Boundary Layer. *Journal of Atmospheric and Oceanic Technology*, *39*(3), 387–402. https://doi.org/10.1175/JTECH-D-21-0126.1

Amaral, J. V., & Guerreiro, R. (2018). Reflections on cost-based pricing and competition-based pricing: The gap may not be so deep. *Revista de Contabilidade e Organizações*, *12*, e143924. https://doi.org/10.11606/issn.1982-6486.rco.2018.143924

Annamalah, S. (2024). The Value of Case Study Research in Practice: A Methodological Review with Practical Insights from Organisational Studies. *Journal of Applied Economic Sciences (JAES)*, *19*(16), 485. https://doi.org/10.57017/jaes.v19.4(86).11

Barber, S., Schubiger, A., Koller, S., Eggli, D., Radi, A., Rumpf, A., & Knaus, H. (2022). The wide range of factors contributing to wind resource assessment accuracy in complex terrain. *Wind Energy Science*, *7*(4), 1503–1525. https://doi.org/10.5194/wes-7-1503-2022

https://doi.org/10.5194/wes-2026-92
Preprint. Discussion started: 18 June 2026

Bechmann, A., Sørensen, N. N., Berg, J., Mann, J., & Réthoré, P.-E. (2011). The Bolund Experiment, Part II: Blind Comparison of Microscale Flow Models. *Boundary-Layer Meteorology*, *141*(2), 245–271. https://doi.org/10.1007/s10546-011-9637-x

Bischoff, O., Hofsäß, M., Clement, D., Schmitt, C., & Cheng, P. W. (2024). Lidar error in complex terrain—Case study based on two measurement campaigns. *Journal of Physics: Conference Series*, *2767*(4), 042032. https://doi.org/10.1088/1742-6596/2767/4/042032

Boventer, J., Bramati, M., Savvakis, V., Beyrich, F., Kayser, M., Platis, A., & Bange, J. (2024). Validation of Doppler Wind Lidar Measurements with an Uncrewed Aircraft System (UAS) in the Daytime Atmospheric Boundary Layer. *Journal of Atmospheric and Oceanic Technology*, *41*(7), 705–723. https://doi.org/10.1175/JTECH-D-23-0127.1

Bretschneider, L., Hankers, R., Schönhals, S., Heimann, J.-M., & Lampert, A. (2021). Wind Shear of Low-Level Jets and Their Influence on Manned and Unmanned Fixed-Wing Aircraft during Landing Approach. *Atmosphere*, *13*(1), 35. https://doi.org/10.3390/atmos13010035

Christoph, K., Paul, M., Jael, S. schweiger, & Jessice, T. (2024). *Levelized Cost of Electricity Renewable Energy Technologies* [Study]. Fraunhofer Institute for Solar Energy Systems ISE. https://www.ise.fraunhofer.de/en/publications/studies/cost-of-electricity.html

Clifton, A., Barber, S., Stökl, A., Frank, H., & Karlsson, T. (2022). Research challenges and needs for the deployment of wind energy in hilly and mountainous regions. *Wind Energy Science*, *7*(6), 2231–2254. https://doi.org/10.5194/wes-7-2231-2022

Clifton, A., Smith, A., & Fields, M. (2016). *Wind Plant Preconstruction Energy Estimates: Current Practice and Opportunities* (Tech. NREL/TP-5000-64735). National Renewable Energy Laboratory. https://docs.nrel.gov/docs/fy16osti/64735.pdf

Dang, J., Xie, X., & Wen, X. (2024). Evaluation of Boundary Layer Characteristics at Mount Si'e Based on UAV and Lidar Data. *Remote Sensing*, *16*(20), 3816. https://doi.org/10.3390/rs16203816

Dörenkämper, M., Olsen, B. T., Witha, B., Hahmann, A. N., Davis, N. N., Barcons, J., Ezber, Y., García-Bustamante, E., González-Rouco, J. F., Navarro, J., Sastre-Marugán, M., Sīle, T., Trei, W., Žagar, M., Badger, J., Gottschall, J., Sanz Rodrigo, J., & Mann, J. (2020). The Making of the New European Wind Atlas – Part 2: Production and evaluation. *Geoscientific Model Development*, *13*(10), 5079–5102. https://doi.org/10.5194/gmd-13-5079-2020

Fernando, H. J. S., Mann, J., Palma, J. M. L. M., Lundquist, J. K., Barthelmie, R. J., Belo-Pereira, M., Brown, W. O. J., Chow, F. K., Gerz, T., Hocut, C. M., Klein, P. M., Leo, L. S., Matos, J. C., Oncley, S. P., Pryor, S. C., Bariteau, L., Bell, T. M., Bodini, N., Carney, M. B., … Wang, Y. (2019). The Perdigão: Peering into Microscale Details of Mountain Winds. *Bulletin of the American Meteorological Society*, *100*(5), 799–819. https://doi.org/10.1175/BAMS-D-17-0227.1

Fu, Y., An, W., Su, X., & Song, B. (2025). Real-Time Wind Estimation for Fixed-Wing UAVs. *Drones*, *9*(8), 563. https://doi.org/10.3390/drones9080563

Gleim, A., Keck, R.-E., & Lund, J. A. (2018). Monte Carlo methods to include the effect of asymmetrical uncertainty sources in wind farm yield assessment. *Wind Engineering*, *42*(6), 624–632. https://doi.org/10.1177/0309524X18780382

Goit, J. P., Shimada, S., & Kogaki, T. (2019). Can LiDARs Replace Meteorological Masts in Wind Energy? *Energies*, *12*(19), 3680. https://doi.org/10.3390/en12193680

https://doi.org/10.5194/wes-2026-92
Preprint. Discussion started: 18 June 2026

Hassani, D. (2023). *Methods, and unmanned aerial systems for obtaining meteorological data* (World Intellectual Property Organization Patent No. WO2023182921A1). https://patents.google.com/patent/WO2023182921A1/en

Henderson, A., Gandoin, R., Marchante, M., Yendole, H., & Méchali, M. (2014, October). Benefits of Measuring the Wind Resource—How Value is Created for the Windfarm. *ResearchGate*. EWEA 2014 Annual Event. https://www.researchgate.net/publication/267099324_Benefits_of_Measuring_the_Wind_Resource_-_How_Value_is_Created_for_the_Windfarm

Hernandez-Negron, C. G., Baker, E., & Goldstein, A. P. (2023). A hypothesis for experience curves of related technologies with an application to wind energy. *Renewable and Sustainable Energy Reviews*, *184*, 113492. https://doi.org/10.1016/j.rser.2023.113492

IEA Wind Task 36. (2022). *Recommended Practice: Forecasting Wind Power – Part 4: Best Practice for the Use of Data in Wind Power Forecasting* (p. 123). International Energy Agency (IEA) Wind TCP. https://iea-wind.org/wp-content/uploads/2022/06/IEAWind_Task36_Recommended_Practice_Part4_1st_Edition_public.pdf

IEC. (2019). *IEC 61400-1: Wind energy generation systems—Part 1: Design requirements: Part 1: Design requirements* (IEC 61400-1; 4.0). https://webstore.iec.ch/en/publication/26423

Indasi, V. S., Lynch, M., McGann, B., Yu, F., Jeanneret, F., & Sutton, J. (2016). WAsP model performance verification using lidar data. *International Journal of Energy and Environmental Engineering*, *7*(1), 105–113. https://doi.org/10.1007/s40095-015-0189-6

Kamdar, I., Ali, S., Taweekun, J., & Ali, H. M. (2021). Wind Farm Site Selection Using WAsP Tool for Application in the Tropical Region. *Sustainability*, *13*(24), 13718. https://doi.org/10.3390/su132413718

Kim, D., Kim, T., Oh, G., Huh, J., & Ko, K. (2016). A comparison of ground-based LiDAR and met mast wind measurements for wind resource assessment over various terrain conditions. *Journal of Wind Engineering and Industrial Aerodynamics*, *158*, 109–121. https://doi.org/10.1016/j.jweia.2016.09.011

Klaas-Witt, T., & Emeis, S. (2022). The five main influencing factors for lidar errors in complex terrain. *Wind Energy Science*, *7*(1), 413–431. https://doi.org/10.5194/wes-7-413-2022

Knoop, S., Bosveld, F. C., De Haij, M. J., & Apituley, A. (2021). A 2-year intercomparison of continuous-wave focusing wind lidar and tall mast wind measurements at Cabauw. *Atmospheric Measurement Techniques*, *14*(3), 2219–2235. https://doi.org/10.5194/amt-14-2219-2021

Kwon, S.-D. (2010). Uncertainty analysis of wind energy potential assessment. *Applied Energy*, *87*(3), 856–865. https://doi.org/10.1016/j.apenergy.2009.08.038

Lee, J. C. Y., & Fields, M. J. (2021). An overview of wind-energy-production prediction bias, losses, and uncertainties. *Wind Energy Science*, *6*(2), 311–365. https://doi.org/10.5194/wes-6-311-2021

Melani, P. F., Di Pietro, F., Motta, M., Giusti, M., & Bianchini, A. (2023). A critical analysis of the uncertainty in the production estimation of wind parks in complex terrains. *Renewable and Sustainable Energy Reviews*, *181*, 113339. https://doi.org/10.1016/j.rser.2023.113339

https://doi.org/10.5194/wes-2026-92
Preprint. Discussion started: 18 June 2026

Menke, R., Vasiljević, N., Wagner, J., Oncley, S. P., & Mann, J. (2020). Multi-lidar wind resource mapping in complex terrain. *Wind Energy Science*, *5*(3), 1059–1073. https://doi.org/10.5194/wes-5-1059-2020

Mora, E. B., Spelling, J., Van Der Weijde, A. H., & Pavageau, E.-M. (2019). The effects of mean wind speed uncertainty on project finance debt sizing for offshore wind farms. *Applied Energy*, *252*, 113419. https://doi.org/10.1016/j.apenergy.2019.113419

Oh, E., & Son, S.-Y. (2019). Shared Electrical Energy Storage Service Model and Strategy for Apartment-Type Factory Buildings. *IEEE Access*, *7*, 130340–130351. https://doi.org/10.1109/ACCESS.2019.2939406

OpenTopography. (2021). *Copernicus GLO-90 Digital Surface Model*. OpenTopography. https://doi.org/10.5069/G9028PQB

Pauscher, L., Vasiljevic, N., Callies, D., Lea, G., Mann, J., Klaas, T., Hieronimus, J., Gottschall, J., Schwesig, A., Kühn, M., & Courtney, M. (2016). An Inter-Comparison Study of Multi- and DBS Lidar Measurements in Complex Terrain. *Remote Sensing*, *8*(9), 782. https://doi.org/10.3390/rs8090782

Rausch, T., Schuchard, M., Cañadillas, B., & Lampert, A. (2022). *One year measurements of vertical profiles of wind speed and wind direction from 40 to 500 m at Clausthal, Harz Mountains, Germany* (p. 41.3 MBytes) [Application/zip]. PANGAEA. https://doi.org/10.1594/PANGAEA.946957

Reuters. (2024, September 17). Germany's onshore wind auction sets record with nearly 3 GW in bids. *Reuters*. https://www.reuters.com/business/energy/germanys-onshore-wind-auction-sets-record-with-nearly-3-gw-bids-2024-09-17/

Schaffarczyk, A. (2014). *Understanding Wind Power Technology: Theory, Deployment and Optimisation* (1st ed). John Wiley & Sons, Incorporated.

Sheehan, H., Traiger, E., Poole, D., & Landberg, L. (2022). Predicting Linearised Wind Resource Grids using Neural Networks. *Journal of Wind Engineering and Industrial Aerodynamics*, *229*, 105123. https://doi.org/10.1016/j.jweia.2022.105123

Soltaninezhad, M., Monsorno, R., & Tondini, S. (2025). A Review of Methods and Challenges for Wind Measurement by Small Unmanned Aerial Vehicles. *Meteorological Applications*, *32*(3), e70065. https://doi.org/10.1002/met.70065

Wildmann, N., Bernard, S., & Bange, J. (2017). Measuring the local wind field at an escarpment using small remotely-piloted aircraft. *Renewable Energy*, *103*, 613–619. https://doi.org/10.1016/j.renene.2016.10.073

Wildmann, N., Hofsäß, M., Weimer, F., Joos, A., & Bange, J. (2014). MASC – a small Remotely Piloted Aircraft (RPA) for wind energy research. *Advances in Science and Research*, *11*(1), 55–61. https://doi.org/10.5194/asr-11-55-2014

Zagubień, A., Wolniewicz, K., & Szwochertowski, J. (2024). Analysis of Wind Farm Productivity Taking Wake Loss into Account: Case Study. *Energies*, *17*(23), 5816. https://doi.org/10.3390/en17235816

Zanaga, D., Van De Kerchove, R., De Keersmaecker, W., Souverijns, N., Brockmann, C., Quast, R., Wevers, J., Grosu, A., Paccini, A., Vergnaud, S., Cartus, O., Santoro, M., Fritz, S., Georgieva, I., Lesiv, M., Carter, S., Herold, M., Li, L., Tsendbazar, N.-E., … Arino, O. (2021). *ESA WorldCover 10 m 2020 v100* (Version v100) [Dataset]. Zenodo. https://doi.org/10.5281/ZENODO.5571936